DEVELOPMENTAL BIOLOGY 173, 428–446 (1996)
ARTICLE NO. 0038

Axis of the *Drosophila* Eye: Graded Expression of the *four-jointed* Gene

Michael H. Brodsky and Hermann Steller

Howard Hughes Medical Institute, Department of Brain and Cognitive Sciences, Department of Biology, Massachusetts Institute of Technology, Cambridge, Massachusetts 02139

Several observations suggest that developing ommatidia in the *Drosophila* eye have distinct dorsal–ventral (d-v) positional identities, despite their morphological uniformity. To identify molecular differences along the d-v axis of the eye, we carried out a systematic screen for P-element insertions that show nonuniform reporter gene expression along this axis. We identified P-element insertions in which *lacZ* expression is activated in dorsal, ventral, or equatorial regions of the disc. These patterns of transcriptional enhancer activity are established early in disc development and are maintained in a size invariant manner during disc growth. Several insertions with an equatorial-to-polar gradient of *lacZ* expression disrupt the *four-jointed* (*fj*) gene which is required for proper leg, wing, and eye development. The *fj* cDNA sequence includes a presumptive internal signal sequence, indicating that *fj* encodes a cell surface or secreted protein. Analysis of the *fj* phenotype and expression pattern in the leg suggests that *fj* is required for cell–cell signaling during disc development.

INTRODUCTION

A fundamental problem in the construction of a complex visual system is how a two-dimensional array of retinal neurons can make topographically organized connections to the brain (Udin and Fawcett, 1988). Gradients and sectors of gene activity have been postulated to explain how apparently uniform groups of cells make position-specific decisions such as cell type determination or axon targeting (Wolpert, 1969; Crick and Lawrence, 1975; Meinhardt, 1982; Bonhoeffer and Gierer, 1984; Gierer, 1987; Baier and Bonhoeffer, 1992; Sanes, 1993). Based on his studies of axon guidance in the vertebrate eye, Sperry proposed that each retinal ganglion cell has a position-specific identity, reflecting a ''pair of tangential gradients'' across the eye (Sperry, 1963). A variety of more recent studies (reviewed in Udin and Fawcett, 1988; Fraser, 1992; Holt and Harris, 1993) has led to the anticipation that genes with graded expression in the eye will be required for visual system development.

A variety of genes have been identified that are expressed in a spatially restricted region of the vertebrate eye (Kaprielian and Patterson, 1994). For example, monoclonal antibody screens have revealed a variety of antigens with nonuniform distribution in the eye. One of these antigens, TOP_{ap}, has been cloned and shown to encode a novel transmembrane protein (Savitt *et al.*, 1995). Other genes with nonuniform expression in the eye include members of the homeobox and TGFβ gene families (Nornes *et al.*, 1990; Deitcher *et al.*, 1994; Rissi *et al.*, 1995) and proteins involved in retinoic acid synthesis (McCaffrery *et al.*, 1993). Analysis of the expression of an Eph receptor tyrosine kinase gene and two Eph receptor ligands suggests that these proteins may directly influence axon guidance in the vertebrate visual system (Drescher *et al.*, 1995; Cheng *et al.*, 1995). Although further genetic and biochemical analysis of these molecules is required to understand their role in eye development, these studies clearly demonstrate that gradients and sectors of gene expression are present in the developing vertebrate eye.

As in vertebrates, growing retinal axons in *Drosophila* can make position-specific responses to guidance cues. During late larval stages, developing photoreceptor neurons send axons to positions along the dorsal–ventral (d-v) axis of the brain that correspond to the d-v position of their cell bodies in the eye (Meinertzhagen, 1973; Trujillo and Melamed, 1973; Fischbach and Dittrich, 1989; Kunes and Steller, 1993). This targeting is not simply a consequence of axon–axon interactions: in genetic backgrounds where most cells are unable to differentiate into photoreceptors, the few neurons that do develop still send axons to approximately the correct d-v positions (Kunes *et al.*, 1993). These

0012-1606/96 $12.00

results suggest that position-specific gene expression may be important for retinal axon guidance in *Drosophila.*

Several additional observations support the idea that there are molecular differences along the d-v axis of the developing *Drosophila* eye. First, developing ommatidia rotate either clockwise or counterclockwise depending on the location of an ommatidium in the dorsal or ventral half of the eye disc (Tomlinson, 1988). Second, among the large number of mutations affecting adult eye structure, several with d-v-specific effects have been described (Morata and Lawrence, 1977; Spencer *et al.,* 1982; Masucci *et al.,* 1990; Lindsley and Zimm, 1992). Finally, the insertion of a P-element carrying the *white* gene into cytological position 24D resulted in a dorsal-specific repression of *white* gene activity (Levis *et al.,* 1985; Hazelrigg and Petersen, 1992). Combined with the axon guidance results, these observations indicate that there may be gradients or sectors of gene expression along the d-v axis of the developing *Drosophila* retina.

Genes with d-v differences in expression may be difficult to identify in traditional genetic screens if they cause lethality prior to photoreceptor differentiation or if they act in partially redundant pathways during eye development. To directly search for transcriptional differences along the d-v axis of the eye disc, we have performed an enhancer trap screen. In this report, we describe the d-v restricted expression patterns of reporter genes inserted at several loci. The combination of sectored and graded expression patterns that we describe indicates that there are many distinct identities along the d-v axis. Analysis of these patterns in younger discs demonstrates that positional differences in transcriptional regulation are present well before the end of disc growth when axon outgrowth and ommatidial rotations occur in the developing eye. We have initiated a molecular and genetic analysis of one of the loci identified in our screen which corresponds to the *four-jointed* (*fj*) gene. This gene has also been recently analyzed in another study (Villano and Katz, 1995). *fj* shows graded expression in the developing eye and appears to encode a novel cell surface or secreted protein. *fj* mutants exhibit defects in eye, leg, and wing morphology. Analysis of the role of *fj* in the development of the proximal–distal axis of the leg suggests that *fj* acts as a cell–cell signaling molecule during *Drosophila* disc development.

MATERIALS AND METHODS

Enhancer Trap Screen

All stocks were obtained from the Bloomington stock center unless otherwise noted. To generate enhancer trap insertions, females containing eight P-*lacW* insertions were crossed to males carrying a genomic source of transposase (Robertson *et al.,* 1988) contained on the third chromosome balancer TMSΔ2-3,Sb. Female progeny containing a P-*lacW* insertion and transposase were crossed to yw males. Male progeny from this cross that have pigmented eyes are the result of a transposition event from an attached X chromosome to a new chromosome. This cross was performed in 240 pools containing 40 ''jumpstarter'' females each. Approximately 300,000 total progeny were generated. Transposition events could be scored in male progeny that did not contain the transposase expressing chromosome. Approximately 15,000 such transposants were examined for non-uniform pigmentation along the dorsal–ventral axis of the adult eye. Stable lines were created from 46 individuals by crossing them to balancer stocks such as yw; CyO/Sco or yw; TM6Ubx/Δ2-3Sb. All of the individuals used to establish lines were from separate pools and therefore arose from independent transposition events.

Imaginal discs from each line were stained for β-galactosidase activity as described previously. Discs were mounted in 70% glycerol and examined on a Zeiss Axiophot microscope. Confocal analysis of β-galactosidase (β-gal) expression was performed as described previously (Winberg *et al.,* 1992). Eye discs and brains were incubated with a 1:100 dilution of rabbit anti-β-gal antibody followed by an incubation with a 1:100 dilution of rhodamine-labeled anti-rabbit antibody and fluorescein-labeled anti-HRP. Imaginal discs and brains were mounted in Vectastain (Vector Laboratories, Inc.) and examined on a Bio-Rad MRC600 confocal microscope using software provided by the manufacturer.

Analysis of Genomic and cDNA Clones from the fj Locus

Genomic DNA adjacent to the fj^{p2} P-element insertion was recovered by plasmid rescue (Steller and Pirrotta, 1986) using an *Eco*RI restriction enzyme digest. This fragment of genomic DNA was used to probe genomic and cDNA libraries. Four overlapping genomic DNA clones were isolated from a λ dash II library prepared from Canton-S DNA (provided by R. Davis). A 6.5-kb *Hin*dIII fragment of genomic DNA was subcloned from one λ clone into pBluescript II (KS^+) for detailed analysis. cDNA clones were isolated from two libraries, a plasmid library prepared from total imaginal disc RNA (provided by N. Brown and F. Kafatos) and a λ gt10 library prepared from eye disc RNA (provided by A. Cowman and G. M. Rubin). The majority of cDNA clones were approximately 1 kb in length; these clones appear to be the result of oligo(dT) priming at a stretch of A residues which also occurs in the genomic sequence. One clone from each library was identified that was greater than 3 kb in length. These clones contain the A-rich region which is present at the 3′ end of the shorter clones.

Sequence analysis of double-stranded plasmid DNA was carried out using Sequenase (United States Biochemical Corp.) according to manufacturer's instructions. Sequence analysis was performed on both strands of two, overlapping cDNA clones from the plasmid library—pfj2 (3.2-kb insert) and pfj13 (1.0-kb insert). Sequence analysis was also performed on one strand of the 6.5-kb genomic subclone in the region corresponding to the cDNA sequences. This genomic fragment contained all but the last 100 bp of the cDNA sequences. Comparison of the cDNA and genomic restric-

tion maps and sequences revealed no introns within the predicted transcript. For any sequence differences between the sequenced clones, an additional genomic or cDNA clone was sequenced in that region. The base found in two of the three clones was used in this report. Within the open reading frame, only a single base pair sequence difference was found; this difference did not result in an alteration of the predicted peptide sequence.

Computer analysis of the cDNA sequence was carried out using the GCG (Genetics Computer Group, Inc.) group of programs. Comparison of cDNA and peptide sequences to available databases was performed using the BLAST and FASTA sequence comparison programs. Comparison of codon usage in the open reading frame to a *Drosophila* codon usage table was performed with the CodonPreference program. Hydropathy analysis was performed using the Kyte-Doolittle algorithm.

Genetic Analysis of fj

A quantitative comparison of *fj* phenotypes was performed on adult leg segments. Each P-element insertion or excision allele was examined in trans to the *Pcl4* deficiency (Lindsley and Zimm, 1992) which includes the cytological region from 55A to 55F. Adults were placed in isopropanol and then transferred to a 1:1 mixture of Canada Balsam and methylsalicylate. Adult legs were removed and mounted in this mixture. A transmitted light image of each leg was acquired on a Bio-Rad MRC600 confocal microscope and segment lengths were measured using software provided by the manufacturer. For each genotype, at least 10 male forelegs were analyzed. Adult eye morphology was examined using both light microscopy and scanning electron microscopy. Deformations of the eye could be observed under a dissecting microscope by examining the curvature of the eye surface from a ventral perspective. For scanning electron microscopy, adult flies were dehydrated through an ethanol series, critical point dried, and coated with gold–palladium. Samples were examined with a scanning electron microscope at the Harvard Museum of Comparative Zoology.

The location and orientation of P-element insertions in the *fj* locus were determined by several methods. Insertions fj^{p1}, fj^{p2}, fj^{p6}, and P55C-I19 were localized to cytological position 55C by *in situ* hybridization to polytene chromosomes. For each stock with an equatorial pattern of β-gal staining in the eye disc, genomic DNA was prepared for PCR and Southern blot analysis. PCR was first performed using one primer (AGCGGCCGCGGTACCACCTTATGTTATTTCATCATG) which recognizes the terminal repeat sequence (underlined) found at both ends of the P-element construct and a second primer from within the cDNA sequence. Using a variety of cDNA derived primers, the insertion site was localized for the nine insertions shown in Fig. 6. Insertion site positions were confirmed using additional cDNA-derived primers to produce PCR products of predicted sizes. Southern blot analysis of each insertion line further confirmed the approximate location of the insertion. The orientations of P-element insertions near the beginning of the cDNA sequence were determined in PCR experiments using a primer (CCTGGCCGTAACCGACCC) that is specific for the *lacZ* sequence contained within the P-element. In combination with a primer derived from the genomic DNA near the insertion, this primer will only produce a product if the *lacZ* gene is adjacent to the genomic primer. These orientations were confirmed in similar experiments using a primer (CCCACGGACATGCTAAGGG) specific to the other end of the P-element sequence.

Reversion of the fj^{p1} and fj^{p2} alleles was accomplished by excision of the associated P-element insertions. Each P-element was mobilized with Δ2-3 (99B), a genomic source of P-transposase (Robertson *et al.*, 1988). Chromosomes that had lost some or all of the P-element insertion were identified by loss of the mini-*white* gene. Reversion of the *fj* phenotype was scored in animals that were homozygous for each excision chromosome. For the fj^{p1} allele, 31 of 49 excision events led to a reversion of the *fj* phenotype. For the fj^{p2} allele, 36 of 63 excision events led to a reversion of the *fj* phenotype.

Deletion alleles of *fj* gene were generated by imprecise excision of the fj^{p2} insertion. This insertion causes a moderate *fj* phenotype. The fj^{p2} insertion was mobilized using Δ2-3 (99B) and 463 chromosomes that had lost some or all of the insertion were identified by loss of the mini-*white* gene. Animals homozygous for these chromosomes were examined for a strong *fj* phenotype. Any chromosomes that had acquired a lethal mutation were crossed to the *Pcl4* deficiency to test if the lethality mapped to the correct genetic region. One excision line, fj^{d3}, had acquired a recessive lethal mutation which failed to complement the *Pcl4* deficiency. This chromosome was shown to have a *fj* mutation by examining the *fj* phenotype of animals heterozygous for this mutation and for the fj^{p1}, fj^{p2}, and the fj^{1} mutations. We do not currently know the gene responsible for the observed lethality. Because this deletion extends past the region included in the *fj* transcript, it is possible that it also removes an adjacent transcript. Alternatively, this chromosome may have gained an addition mutation at a more distant location. Four excision chromosomes that had not acquired lethal mutations had strong *fj* mutations. Each of these failed to complement the fj^{1} and fj^{p1} alleles. The genomic DNA surrounding the initial fj^{p2} insertion site was examined by Southern analysis. Two of the viable excisions alleles did not appear to remove a substantial amount of genomic DNA. Both of these still had some P-element sequences remaining. Two of the viable excision alleles, fj^{d1} and fj^{d2}, had deletions which included some of the transcribed region adjacent to the P-element insert. The lethal excision allele, fj^{d3}, removed all of the identified transcribed region.

Wholemount in Situ Hybridization to Imaginal Discs

In situ hybridization to imaginal discs was performed using digoxigenin-labeled probes (Tautz and Pfeifle, 1989). Sense and antisense RNA probes were generated from a subclone of genomic DNA which extends from the begin-

ning of the transcribed region to the first *Eco*RI site at base-pair 530 in the cDNA. Probes were synthesized using the Boehringer RNA labeling kit and the manufacturer's instructions. Discs were dissected from larvae and fixed for 1 hr in 4% paraformaldehyde. Discs were washed in PBS and incubated in 90% methanol, 10% 0.5 *M* EGTA for 1 min. Discs were rehydrated in a series of methanol: PBT (PBS plus 0.1% Tween 20) washes. Discs were treated with 10 mg/ml proteinase K for 5 min and then washed with PBT. Subsequent fixation, hybridization, and signal detection were carried out essentially as described (Tautz and Pfeifle, 1989). Discs were mounted in 70% glycerol and examined on a Zeiss Axiophot microscope.

RESULTS

Enhancer Trap Screen

We used two genes, *lacZ* and mini-*white*, as reporters for patterned enhancer activity in the eye (Fig. 1A). The P-*lacW* P-element construct (Bier *et al.*, 1989) contains a fusion of the *lacZ* gene with part of the transposase gene. The weak promoter provided by the transposase gene is readily activated when the P-element inserts in a genomic region containing sequences with transcriptional enhancer activity. The *lacZ* expression seen in enhancer trap lines often reflects the spatial and temporal transcription pattern of a gene adjacent to the P-element insertion (Bellen *et al.*, 1989; Bier *et al.*, 1989; Wilson *et al.*, 1989). In addition to the *lacZ* reporter gene, this construct also contains the mini-*white* gene. This gene serves as a genetic marker for the P-element, but several characteristics (Pirrotta and Rastelli, 1994) also make it suitable as a reporter for patterned enhancer activity in the developing eye; in particular, the mini-*white* gene acts cell autonomously and its expression level is sensitive to the action of nearby enhancer sequences.

This two-reporter enhancer trap screen is outlined in Fig. 1B. Because mini-*white* expression can be quickly assayed in the adult eye, we were able to carry out an extensive, yet relatively rapid, screen for individuals with patterned reporter gene expression. Only those individuals with non-uniform eye pigmentation were used to generate lines for further analysis. Larvae from each line were dissected and tested for *lacZ* expression in the disc by staining for β-gal activity. Of 15,000 individuals with new enhancer trap insertions, 46 had nonuniform pigmentation in the d-v axis of the eye and 18 of those had a similar pattern of *lacZ* expression in the eye disc. The remaining lines had little or no *lacZ* expression in the disc. No line showed a pattern of *lacZ* expression that was distinct from the pattern of mini-*white* expression.

Reporter Expression Patterns

In the 18 lines with β-gal staining in the eye disc, four types of *lacZ* expression patterns were observed. All insertions with the same type of expression pattern were found

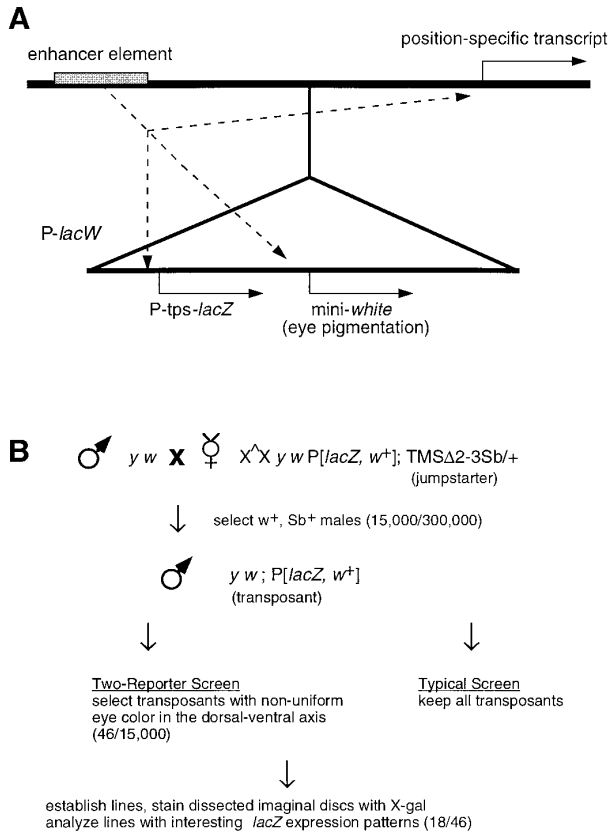

FIG. 1. An enhancer trap screen using two reporter genes. To identify molecular differences among ommatidia at identical developmental stages, an enhancer trap screen was performed using both the *lacZ* and mini-*white* genes as reporters of enhancer activity. (A) The temporal and spatial pattern of transcription of many genes is controlled by the action of transcriptional enhancer elements which can act on promoter elements at a distance. When a P-element construct inserts near such an enhancer element, the expression of reporter genes having minimal promoter elements can be controlled by the enhancer sequences. The temporal and spatial expression pattern of the *lacZ* gene is assayed with a histological stain for the β-galactosidase protein. The spatial, but not temporal, expression pattern of the mini-*white* gene in the developing eye is assayed by examining adult eye color. (B) Comparison of the two-reporter screen with a typical single reporter screen. P-elements are mobilized in ''jump-starter'' animals by the introduction of a genomic source of transposase (Δ2-3). Individuals with new P-element insertions are identified by the presence of a P-element specific marker, the mini-*white* gene, in progeny that did not inherit the chromosome containing the original P-element insertion site. In the screen shown, the original insertions are on an attached X chromosome (X^X) which will not be present in any of the male progeny. In a typical screen, all the F1 males expressing a functional mini-*white* gene are used to establish lines for further analysis. In the two-reporter screen, only those transposants with a particular pattern of mini-*white* gene expression are used to establish lines for further analysis. Of approximately 15,000 transposants examined, 46 with dorsal–ventral-specific patterns of eye pigmentation were saved.

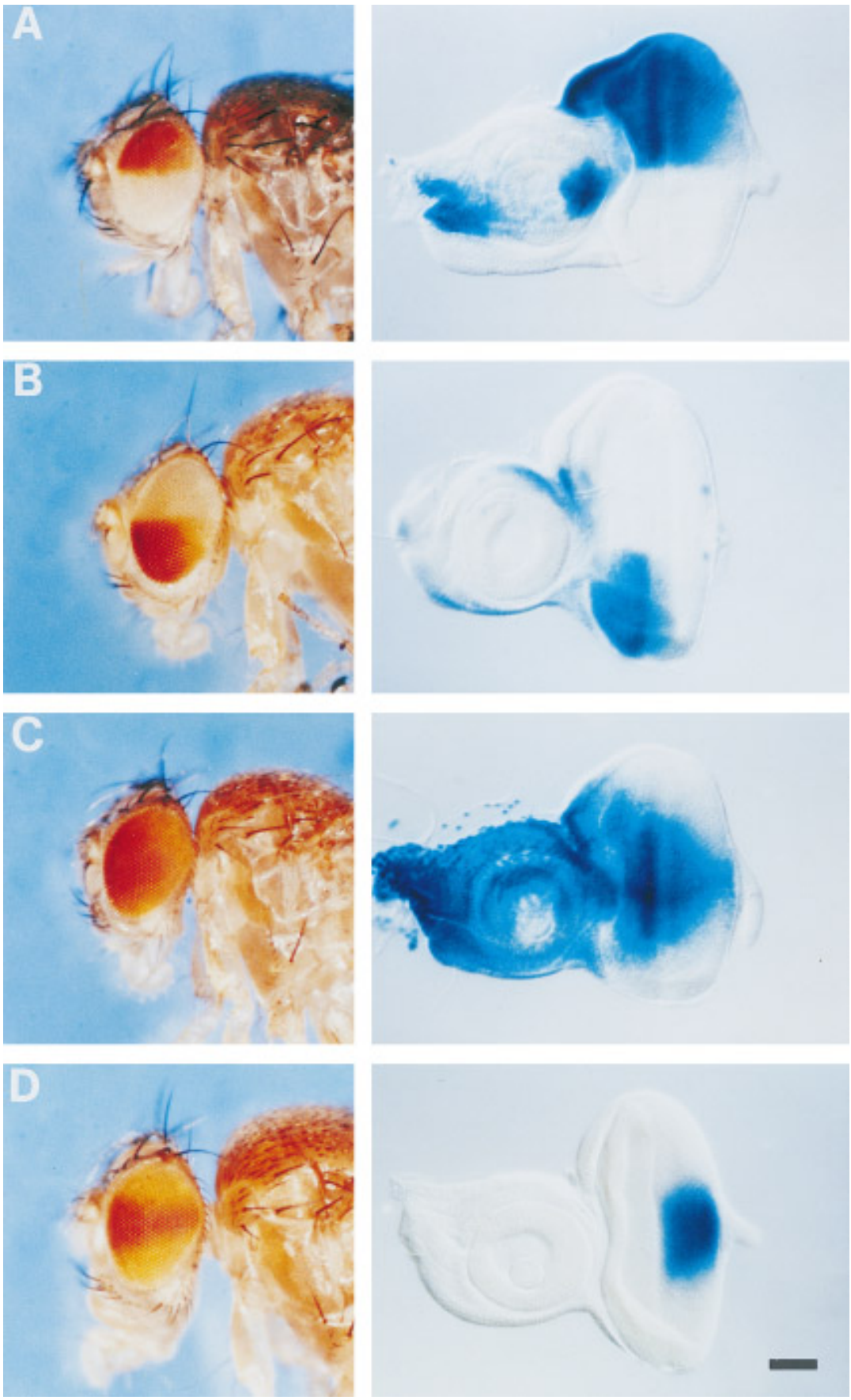
A
B
C
D

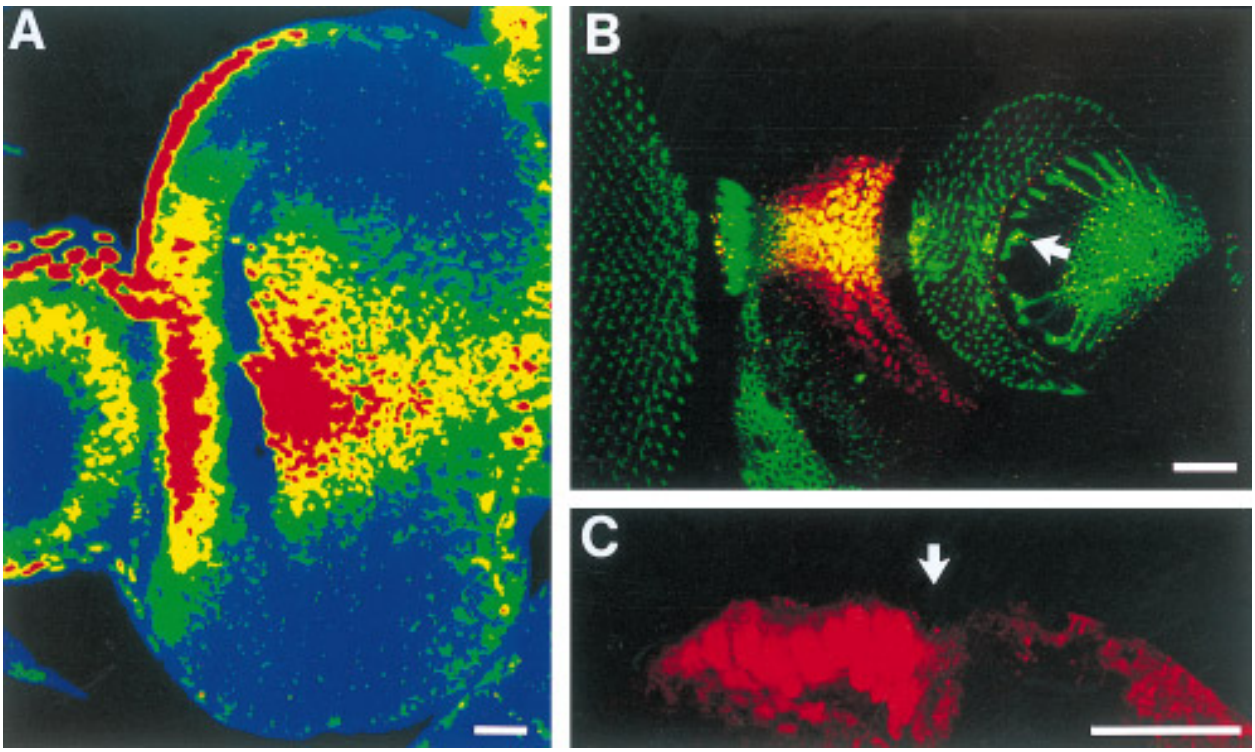

FIG. 3. Confocal analysis of *lacZ* expression. Third instar eye discs and brains were dissected from a line with an enhancer trap insertion at 55C, stained with anti-β-galactosidase and anti-HRP antibodies, and viewed with a confocal microscope. Anti-HRP antibodies recognize neuronal cell membranes (Jan and Jan, 1982), including axons. For (A) and (B), anterior is left and dorsal is up. For (C), anterior is left and lateral is up. Scale bars: (A) 15 μm, (B and C) 25 μm. (A) A gradient of *lacZ* expression in the eye disc. Different levels of fluorescence intensity were assigned different colors using the histogram option of the confocal microscope software package. The relative intensity ranges and corresponding colors are as follows: 180–255, red; 120–180, yellow; 70–120, green; 10–70, blue; 0–10, black. (B, C) *lacZ* expression in the developing lamina. The nuclei of *lacZ* expressing cells are shown in red and neuronal cell membranes, including axons, are shown in green. Detailed descriptions of similar views of the developing lamina have been provided previously (Winberg *et al.*, 1992; Kunes *et al.*, 1993). In a lateral view of the developing eye disc and brain (B), the developing photoreceptors in the eye disc can be seen on the left and an optical cross section through their axons as they pass through the developing lamina can be seen as a crescent on the right. The approximate position of the dorsal–ventral midline of the developing lamina is indicated (arrow). Expression of the *lacZ* reporter is found in cells anterior to the innervated region of the lamina. These cells will be induced to become part of the lamina by the arrival of additional photoreceptor axons. Within the preinnervated region of the lamina, the highest levels of reporter expression are found in a region ventral to the dorsal–ventral midline. In a horizontal view of the developing lamina (C), *lacZ* expression is found anterior to the lamina furrow (arrow), in the region where the most recently differentiated retinal axons arrive. The position of the *lacZ* expressing cells indicates that they will give rise to lamina neurons.

FIG. 2. Patterns of mini-*white* and *lacZ* reporter gene expression. Enhancer trap insertions at four loci were isolated that had nonuniform *lacZ* expression along the d-v axis of the eye. Examples of mini-*white*-dependent adult eye pigmentation (left) and β-galactosidase staining in late third instar eye discs (right) are shown for one line from each locus. Other lines from a given locus have similar patterns of reporter gene expression, but may have weaker levels of reporter gene expression. Note that in addition to the d-v differences seen in these lines, reporter expression is also nonuniform along the anterior–posterior axis; these differences are probably caused by changes in gene expression as ommatidial differentiation proceeds. For all panels, anterior is left and dorsal is up. Scale bar for eye discs, 50 μm. (A) Dorsal-specific expression. Four lines were recovered with insertions at cytological position 69D which showed dorsal-specific expression of mini-*white* and *lacZ* in the eye. Examples are shown from insertion P69Df7. (B) Ventral-specific expression. Three lines were recovered with insertions at cytological position 24D which showed ventral-specific expression of mini-*white* and *lacZ* in the eye. A P-element insertion at this locus was previously identified in which expression of an intact *white* gene was repressed in a dorsal region of the eye (Levis *et al.*, 1985; Hazelrigg and Petersen, 1992). Examples are shown from insertion P24De13. (C) Equatorial-specific expression. Ten lines were recovered with insertions at cytological position 55C which showed equatorial-specific expression of mini-*white* and *lacZ* in the eye. Nine of these lines also show nonuniform expression in the developing brain (see Fig. 3B). Examples are shown from insertion fj^{p1}. (D) Equatorial-specific expression, posterior to the morphogenetic furrow. The original P-element insertion at cytological position 53C only showed faint *lacZ* expression, but lines with stronger reporter gene expression were generated by mobilization and reinsertion of this P-element (data not shown). These lines showed equatorial expression of mini-*white* in the eye and equatorial expression of *lacZ* in cells posterior to the morphogenetic furrow in the eye disc. Examples are shown from insertion P53Cm100.

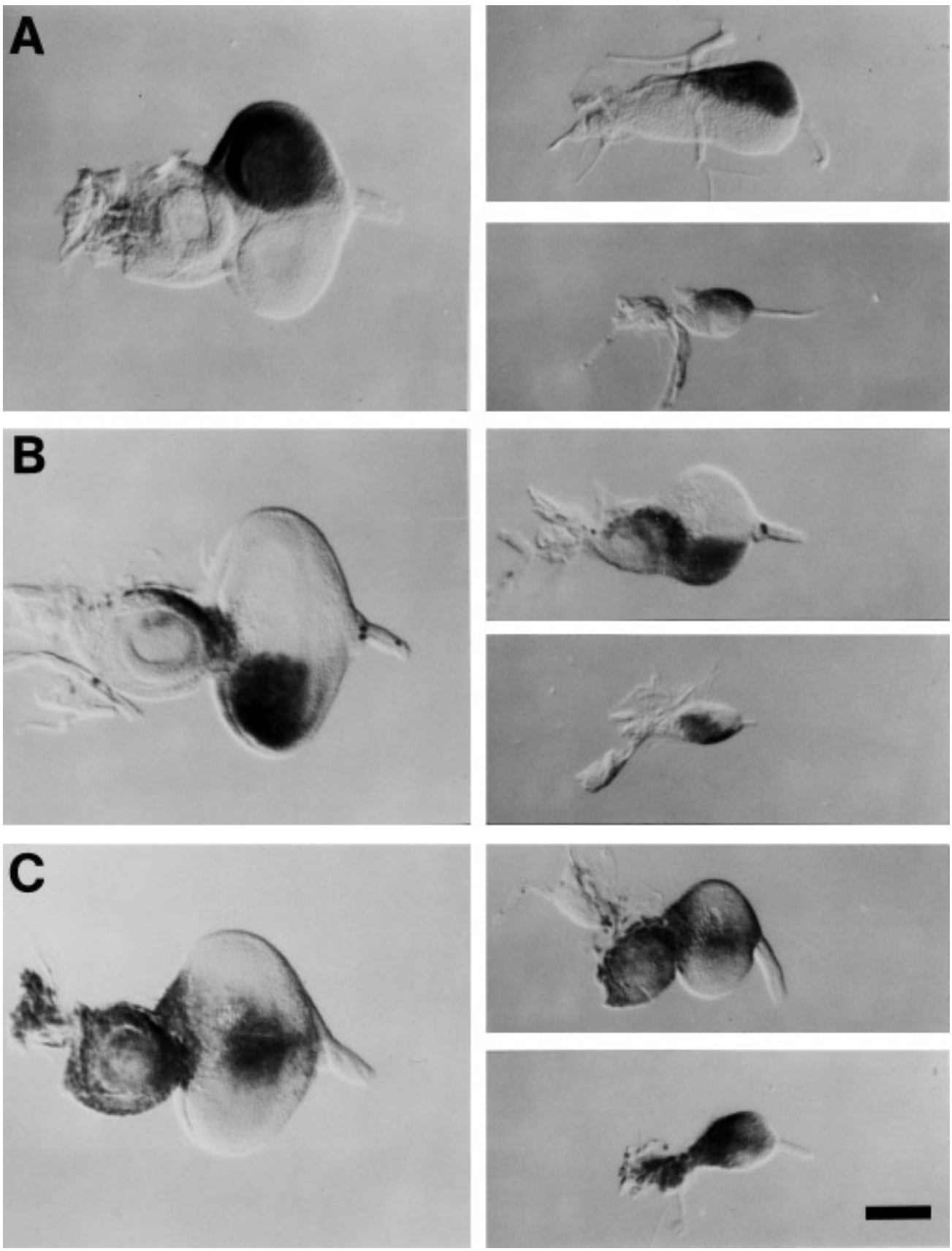
A
B
C

TABLE 1
Summary of Enhancer Trap Lines with Nonuniform Expression of mini-*white* and *lacZ* along the Dorsal–Ventral Axis of the Eye

Cytological location	Number of insertions	Eye disc expression	Phenotypes	Comments
69D	4	Dorsal	3 viable, 1 lethal (P69D-f7)	Fails to complement *Dichaete*[1]
24D	4	Ventral	All viable	Same location as described by Hazelrigg[a]
55C	10	Equatorial	See Figs. 7 and 8	*four-jointed*, also expressed in developing brain
53C	1(+)[b]	Equatorial[c]	Viable	Expression in eye is *glass*-dependent

Note. Reporter expression of one example from each locus is shown in Fig. 2. Except for insertions in the *four-jointed* gene, animals homozygous for viable insertions did not show striking defects in the external structure of adult tissues.

[a] See Levis *et al.,* 1985; Hazelrigg and Petersen, 1992.

[b] Because the original insertion at this locus (P53C-e2) exhibited weak reporter gene expression, local P-element hopping was used to generate another line (P53C-m100) with stronger reporter gene expression. In a separate screen using an enhancer trap construct containing the *rosy* gene, we isolated an additional insertion (P53C-b347) at this locus.

[c] In this line, eye disc expression is only found posterior to the morphogenetic furrow.

to be at the same cytological position in the genome. Although all P-element insertions at a single locus had a similar pattern of *lacZ* expression, they often differed in the level of expression. In Fig. 2, an adult eye and a third instar eye–antennal disc stained for *lacZ* expression are shown for one strongly staining line from each locus. There is a clear spatial correspondence between adult eye pigmentation and β-gal staining. Table 1 summarizes the lines described in this section.

P-element insertions at cytological positions 69D and 24D gave rise to mini-*white*-dependent pigmentation that was restricted to either dorsal or ventral regions of the eye, respectively (Figs. 2A and 2B). For both lines shown, the complete absence of pigmentation in part of the eye suggested that expression of the mini-*white* reporter gene was partly regulated by negative enhancer elements or silencers. Consistent with this interpretation, previous studies have found that expression of an intact *white* gene inserted at 24D was repressed in the dorsal region of the eye (Levis *et al.*, 1985; Hazelrigg and Petersen, 1992). In the lines we isolated, expression of the *lacZ* reporter was also restricted to either a dorsal or ventral region of the third instar eye disc. Interestingly, although most cells in the disc were contained within either the dorsal or ventral regions defined by these enhancer trap lines, a thin stripe of cells near the d-v midline did not express the *lacZ* reporter gene in either line.

Enhancer trap insertions at 55C gave rise to a gradient of *lacZ* expression in the eye disc. Different insertions isolated at 55C all show pigmentation and β-gal staining in a broad, equatorial region of the eye (Fig. 2C). However, the region of the disc with detectable β-gal staining is larger in lines that show higher levels of *lacZ* expression. This observation suggests that activation of reporter gene expression might be graded along the d-v axis. We used confocal microscopy to visualize the changes in β-gal levels across the eye disc (Fig. 3A). The highest levels of β-gal are detected near the d-v midline of the disc and decreasing levels are observed toward either the dorsal or ventral pole. Combined with the dorsal- and ventral-specific patterns described above, this graded pattern of reporter expression suggests that many positions within a single d-v column are transcriptionally distinct. Based on these observations, it appears that the d-v positional identity of a cell in the eye disc could be specified based on its distance from the d-v midline and its inclusion in the dorsal or ventral region of the eye disc.

An insertion at 53C gave rise to an equatorial band of mini-*white*-dependent pigmentation (Fig. 2D). Along the d-v axis, *lacZ* expression in this line was strongest in an equatorial region of the eye disc. This expression decreases in a graded fashion at the dorsal and ventral edges. Unlike the other patterns described, *lacZ* expression in this line is only found posterior to the morphogenetic furrow and is restricted to developing photoreceptor cells. This expression is dependent on the *glass* gene (data not shown) which encodes a transcription factor required for the expression of many photoreceptor-specific genes and for retinal axon guidance (Moses *et al.*, 1989; Moses and Rubin, 1991; Selleck and Steller, 1991; Kunes *et al.*, 1993). This line demonstrates that region-specific enhancer activity is also present in retinal cells as they differentiate into photoreceptor neurons and send axons toward the brain.

FIG. 4. Size-invariant patterns of reporter expression during disc growth. β-Galactosidase staining is shown for mid third instar, early third instar, and mid to late second instar eye discs. For each line shown, the pattern of reporter gene expression is maintained during several stages of disc growth. For all panels, anterior is left and dorsal is up. Scale bar, 50 μm. (A) Dorsal-specific expression in eye discs from a stock with the P69Df7 insertion. (B) Ventral-specific expression in eye discs from a stock with the P24De13 insertion. (C) Equatorial-specific expression in eye discs from a stock with the fj^{p2} insertion.

Size Invariance of Patterned Enhancer Activity

To examine if these position-specific differences in enhancer activity existed prior to late third instar, we examined *lacZ* expression in second to mid third instar larval eye discs. In a line that had dorsal-specific *lacZ* expression in the late third instar disc, *lacZ* expression was restricted to a dorsal region of the eye disc in second instar and this restriction was maintained through mid third instar (Fig. 4A). Likewise, a line with ventral-specific *lacZ* expression in late third instar exhibited ventral-specific expression at earlier stages (Fig. 4B). These observations are consistent with the previous suggestion that cells in dorsal and ventral regions of the eye arise from separate cell populations (see Discussion). In another line, *lacZ* expression is highest in an equatorial region of the third instar eye disc. Again, the pattern of *lacZ* expression in younger discs is qualitatively similar to that seen in the late third instar disc (Fig. 4C). These results demonstrate that d-v-specific patterns of enhancer activity are established prior to third instar and are maintained until cell division in the disc has ended.

Graded Expression of an Endogenous Transcript

Patterns of *lacZ* expression demonstrate that enhancers of transcriptional activation exist that have differential activity along the d-v axis of the eye. To confirm that an endogenous gene is controlled by one of these enhancers, we have characterized a transcript adjacent to the insertions at cytological position 55C. These insertions were chosen because of their striking gradient of *lacZ* expression in the eye disc (Fig. 3) and because some of the insertions disrupt the development of adult tissues (see below). As described in the next section, the transcript we have identified is required for the function of a previously identified gene, *four-jointed*.

Genomic DNA adjacent to the P-element insertions was isolated (Fig. 5); a fragment of this DNA hybridizes to a transcript of approximately 3.5 kb (data not shown). We used this fragment to isolate overlapping cDNA clones which, when combined, predict a 3.6-kb transcription unit. The cDNA sequences begin at the site of the fj^{p2} P-element insertion and continue just past the end of the *Hin*dIII genomic fragment shown (Fig. 5). Comparison of cDNA restriction maps and sequences to the genomic restriction map and sequence indicates that there are no introns in this transcript. We have mapped the approximate insertion sites for 9 of 10 insertions in this locus: 2 are located within the transcribed region, 1 is 3 kb upstream, and 6 are just upstream of the 5′ end of the longest cDNA. The clustering of P-elements near the likely transcriptional start site is consistent with the previous observation that P-elements

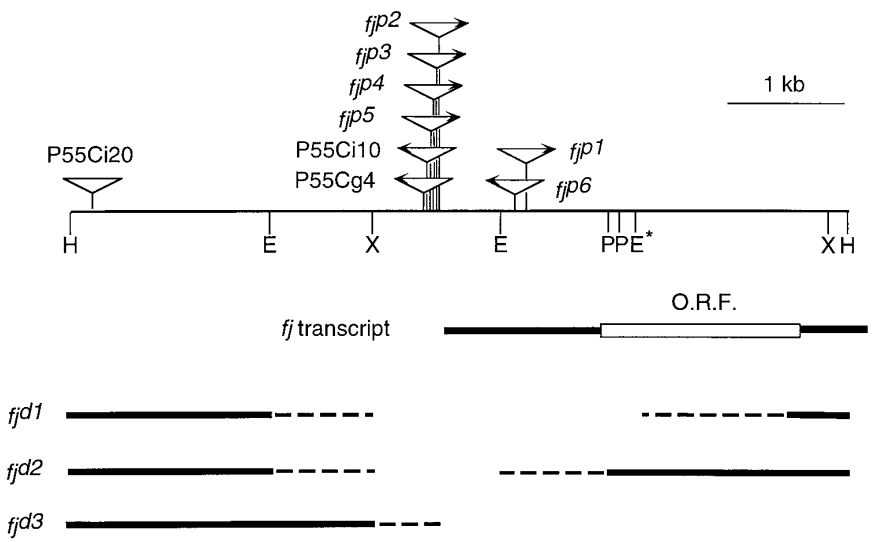

FIG. 5. Molecular characterization of *four-jointed*. The positions of P-element insertions, the transcribed region, and deletion mutations are shown on a 6.5-kb genomic fragment. Insertions that result in an adult leg phenotype are referred to by their *four-jointed* allele designation. The restriction sites shown are as follows: H, *Hin*dIII; E, *Eco*RI; X, *Xba*I; P, *Pst*I. The site marked with an asterisk is polymorphic between the genomic clone and the chromosome containing the fj^{p2} insertion. The P-element insertion sites are depicted by a triangle and a vertical line. The orientation of the P-element insertion is indicated by an arrow within the triangle. The arrow is pointed in the direction of transcription for the *lacZ* gene. The orientation of insertion P55Ci20 was not determined. The location of the cDNA sequences is indicated below the restriction map. Sequencing and restriction mapping do not reveal any introns in the transcribed region. The direction of transcription is from left to right in this figure. The region of the cDNA sequences that form an open reading frame is indicated as an open box. At the bottom, the regions of genomic DNA missing in various deletion alleles are depicted as breaks in a line. The dashed lines indicate the region to which the deletion breakpoints have been localized. One breakpoint for deletion fj^{d3} occurs to the right of the region depicted.

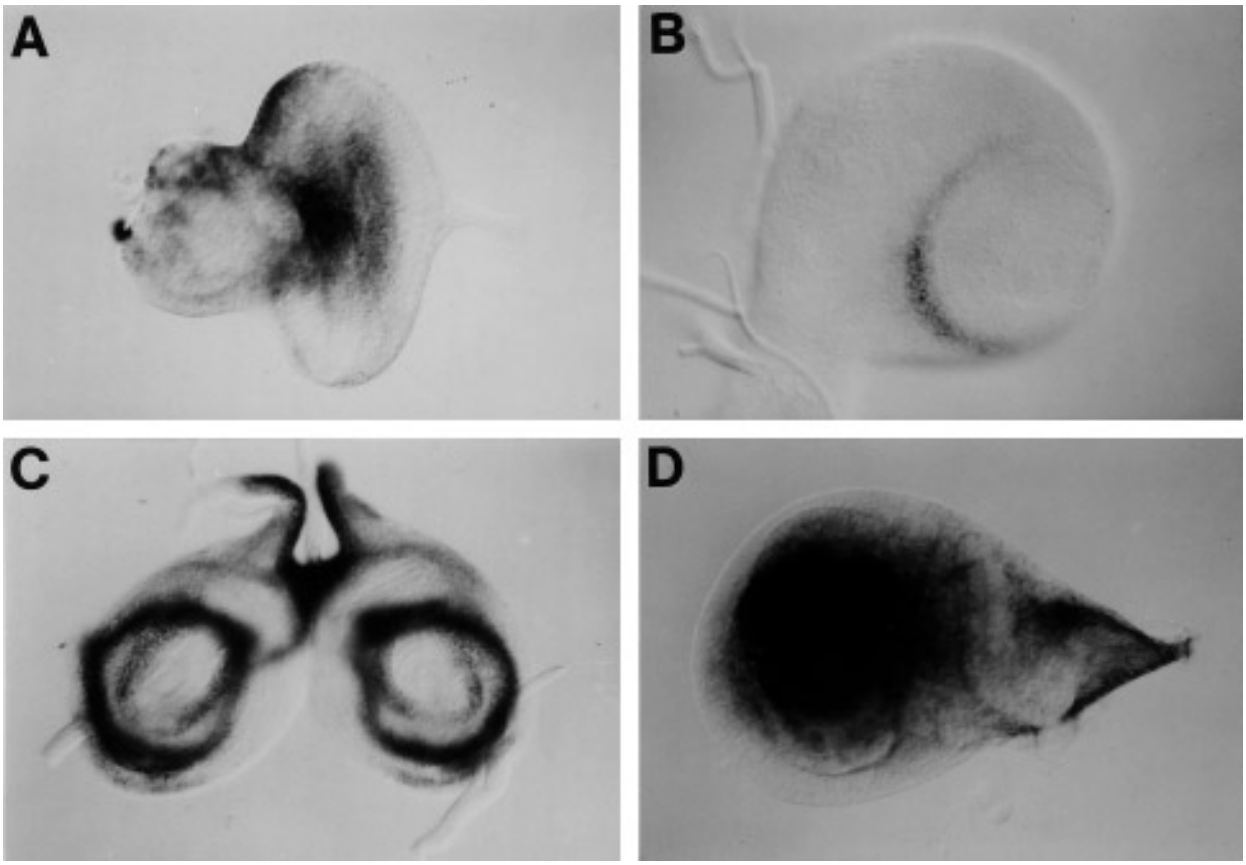

FIG. 6. Distribution of the *four-jointed* transcript in third instar tissues. *four-jointed* RNA distribution was detected in late third instar discs and brains by *in situ* hybridization with a digoxigenin-labeled RNA probe. For (A) and (B), anterior is left and dorsal is up. Expression is shown for an eye disc (A), a developing brain (B), a pair of leg discs (C), and a wing disc (D).

often insert into the promoter regions of genes (Engels, 1989).

In situ hybridization with a probe derived from DNA encoding part of this transcript demonstrates that the RNA distribution matches the expression pattern of the *lacZ* reporter in several discs. Transcript levels in the eye disc are highest near the equator, lower in an intermediate region, and very low in the dorsal or ventral polar regions (Fig. 6A). In the developing brain, the transcript is found in cells immediately anterior to the innervated region of the lamina (Fig. 6B). Confocal analysis of *lacZ* expression in the brain indicates that this expression is confined to lamina neuronal precursor cells (Figs. 3B and 3C). Along the d-v axis of the brain, transcript levels are somewhat higher in a region ventral to the midline and are lower near both the dorsal and ventral poles. Expression in the wing disc is found in a large central region including the wing pouch which gives rise to the adult wing (Fig. 6D). In the leg disc, the transcript is found in two concentric circles (Fig. 6C). The innermost ring of expression is a region of the disc that will give rise to the first tarsal segment of the leg. Examination of several enhancer trap lines with high levels of *lacZ* expression in the leg did not reveal any regions of lower level expression in this region of the leg (data not shown). This expression pattern suggests that this transcript might play a role in the development of the proximal–distal axis of the leg. As described below, the phenotypes associated with mutations that affect this transcript are consistent with this conclusion.

Genetic Analysis of four-jointed

To probe the function of this transcript during development, we attempted to identify mutations that removed its activity. We examined animals homozygous for each P-element insertion. All of the insertions are homozygous viable. Because of the transcript distribution in imaginal discs, we examined eyes, legs, and wings in adults homozygous for each insertion. Compared to wild-type, adults homozygous for the fj^{P1} insertion have much shorter legs, with four tarsal segments instead of five (Figs. 7A and 7C). They also show a decrease in wing length that can be seen by examining the distance between the two cross-veins (Figs. 7D and 7F). Animals homozygous for several other insertions are missing one tarsal segment (Fig. 7B), but the overall leg and wing lengths are largely unaffected. The phenotypes

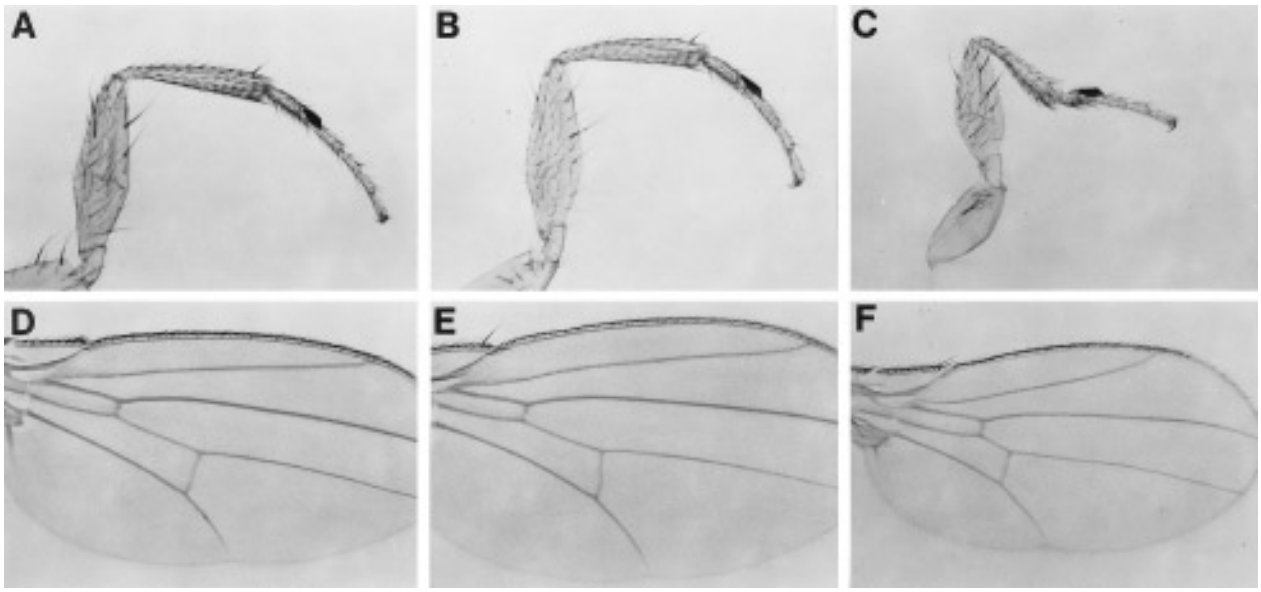

FIG. 7. Leg and wing phenotypes in *four-jointed* insertion alleles. Male forelegs (A–C) and wings (D–F) from wild-type (A, D), fj^{p2} (B, E), and fj^{p1} (C, F) animals. For all panels, distal is right. In the wild-type leg, the five small tarsal segments at the distal end of the leg can be seen (A). fj^{p2} is a moderate *four-jointed* allele caused by a P-element insertion at the 5′ end of the *four-jointed* transcript. In animals homozygous for this insertion, the length of most of the leg segments is unaffected, but there are only four tarsal segments instead of five. The decrease in the number of tarsal segments appears to be due to the fusion of the second and third tarsal segments. fj^{p1} is a stronger *four-jointed* allele caused by a P-element insertion within the *four-jointed* transcript. In animals homozygous for this insertion, the second and third tarsal segments are again fused into a single segment (C). In addition, several other leg segments, including the tibia, femur, and first tarsal segment, are significantly decreased in length. Another phenotype associated with this insertion is a decrease in wing size compared with wild-type. This difference is most readily seen by comparing the distance between the two cross-veins in wild-type (D) and fj^{p1}(F) wings.

associated with the fj^{p1} insertion resemble those described in animals mutant for a gene previously mapped to the same genetic location, *four-jointed* (Lindsley and Zimm, 1992). In agreement with this observation, the insertion alleles fj^{p1} and fj^{p2} both fail to complement the originally described fj^{1} allele. Both of these insertions were remobilized to generate chromosomes that no longer contained the P-element insertion (see Materials and Methods). A high percentage of these chromosomes no longer carried a *fj* mutation. These revertants verify that the P-element insertions are directly responsible for the *fj* mutations. Several insertions with moderate *fj* phenotypes, including fj^{p2}, are found in the putative promoter region of the transcript described above. The insertion with the strongest phenotype, fj^{p1}, occurs within the transcript.

The clustering of P-element insertions associated with *fj* mutations directly adjacent to or within this transcript strongly implicates that it is required for the function of the *fj* gene, but an alternative possibility is that the insertion of a 10-kb P-element disrupts the function of a more distant transcript that is required for *fj* function. To generate additional *fj* alleles which did not contain P-element sequences, we remobilized the fj^{p2} insertion and screened for imprecise excision events that caused phenotypes resembling the fj^{p1} phenotype. Several deletions were identified that had a strong *fj* phenotype, but no longer contained any P-element sequences (Fig. 5). Deletion allele fj^{d1} removes approximately 4 kb of DNA surrounding the fj^{p2} insertion site, including the beginning of the open reading frame found in the transcribed sequence. Deletion allele fj^{d2} removes approximately 2 kb of DNA flanking fj^{p2}, indicating that sequences important for *fj* function are in the immediate vicinity of this insertion. Both the fj^{d1} and fj^{d2} deletion alleles are homozygous viable and are associated with strong *fj* phenotypes when homozygous and in combination with an independently generated deficiency for 55C, *Pcl4*. Together, the molecular analysis of insertion and deletion mutations indicate that this transcript is required for *fj* function.

A quantitative analysis of several alleles indicates that *fj* has variable effects on the longitudinal growth of different tarsal segments in the leg. Previous analysis of the fj^{1} allele indicated that the *fj* gene was required for longitudinal growth (i.e., along the proximal–distal axis) but not circumferential growth (i.e., along the radial axis) in the leg (Waddington, 1943; Tokunaga and Gerhart, 1976). Consistent with this conclusion, we have not observed defects in circumferential growth associated with any of the *fj* alleles we have examined. To compare the effects of different *fj* alleles on longitudinal growth, we have measured leg segment lengths in mutant animals (Fig. 8). The only defect we have

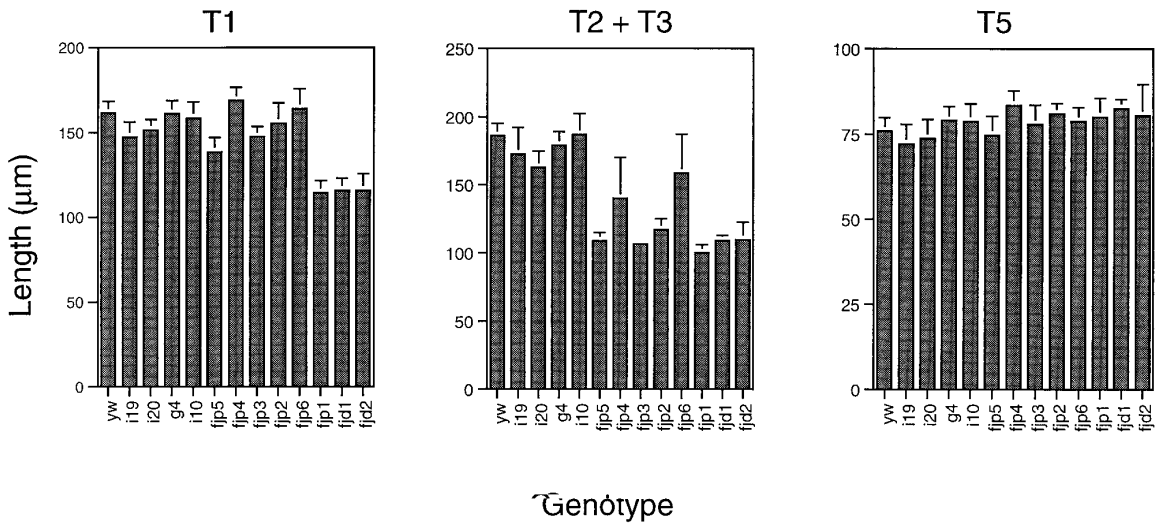

FIG. 8. Quantitative comparison of *four-jointed* alleles. Leg segment lengths were measured (see Materials and Methods) for each of the P-element insertions at 55C and for the two viable deletion alleles described in the text. Each insertion or deletion was examined in trans to the *Pcl4* deficiency which includes the 55C cytological region. Because all of the insertions and deletions were created in a *yellow, white* (*yw*) background, *yw* crossed to the *Pcl4* deficiency was used as the wild-type control. The fj^{p1} insertion allele and the deletion alleles showed significant decreases in the length of tarsal segment one. The lengths of the second and third tarsal segments were added together in animals that did not have a fused segment. Many of the insertions resulted in fusion of these segments. None of the insertions or deletions had a significant effect on the length of the fifth tarsal segment.

detected in weak alleles of *fj* is the fusion of the second and third tarsal segments into a single segment (Figs. 7 and 8). The weakest *fj* alleles, fj^{p5} and fj^{p6}, show incomplete penetrance for this phenotype, resulting in a large deviation for the combined length of the second and third segments. Strong alleles of *fj* also have a reduction in the length of the first tarsal segment (Fig. 8), as well as the tibia and femur (data not shown). None of the mutations affect the length of the most distal segments, the fourth and fifth tarsal segments (Fig. 8).

A previous analysis of the original fj^1 mutation did not address the possibility that this strong allele still produces some, but not wild-type levels, of the *fj* gene product (Tokunaga and Gerhart, 1976); thus, it could not be ruled out that *fj* was required for disc growth in general and that the specific growth defects observed were the result of a partial loss of *fj* function. The fj^{d1} allele described here is unlikely to produce a functional protein product from the *fj* transcript. This deletion removes all of the 5′ untranslated region and at least the first 100 aminio acids of the open reading frame including a putative signal sequence, predicted to direct the encoded protein to the cell surface (see below). Thus, the phenotype associated with this allele probably represents a null phenotype for this transcript. Like the previously characterized fj^1 allele, this mutation affects the first three tarsal segments, but not the forth and fifth, confirming that *fj* is specifically required for longitudinal growth of a subset of tarsal segments. We have not repeated the mosaic analysis performed previously (Tokunaga and Gerhart, 1976) because large mutant clones in the leg include multiple tarsal segments (see Discussion).

We also examined the effect of strong *fj* mutations on eye development. In contrast to the differences seen in adult leg morphology, the adult eyes of animals with *fj* mutations are not significantly reduced in size compared to wild-type. However, we have observed deformations of the eye surface in some of these animals (Fig. 9). Although this phenotype occurs with incomplete penetrance and variable expressivity, we have observed it in animals containing a variety of independently generated *fj* mutations, but never in siblings from the same crosses that are heterozygous for *fj* mutations. The epigenetic factors affecting the penetrance and expressivity of this phenotype are unclear. When examined by scanning electron microscopy, most *fj* animals have eyes with either wild-type curvature or slight indentations. For Fig. 9, we have selected examples that demonstrate the range of observed defects from nearly wild-type (9B) to extreme cases with multiple indentations of the eye surface (9D). In sections of these eyes, both ommatidial rotations and the arrangement of photoreceptor rhabdomeres within individual ommatidia appear normal. In addition, the underlying lamina, which is dependent on photoreceptor axon input for proper development (Selleck and Steller, 1991), appears normal at this level of resolution. In the third instar eye disc and brain, we have not observed any dramatic defects in the proper spacing of differentiating ommatidia, the arrangement of retinal axons as they grow into the brain, or the size and morphology of the disc itself. In addition, *four-jointed* mutations did not alter the expression of another equatorial enhancer trap line, P53Cm100 (shown in Fig. 2D). Although the deformed eye phenotype may reflect an interesting global defect in eye formation, its low penetrance and variability make a more detailed analysis of the

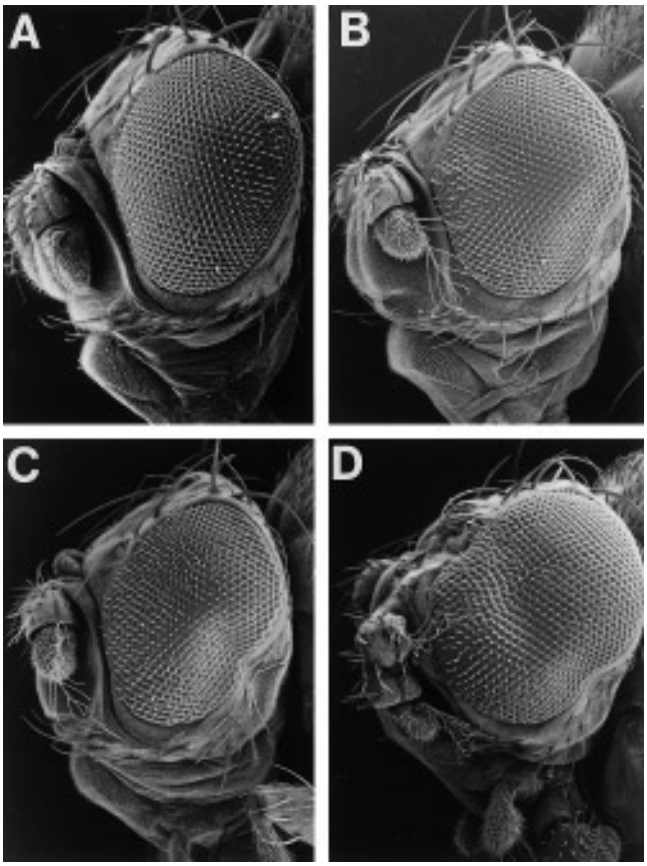

FIG. 9. Eye deformities in *four-jointed* animals. Scanning electron micrographs of wild-type (A) and selected *four-jointed* (B–D) adult eyes. The wild-type eye is composed of approximately 800 ommatidia which are arranged in an extremely regular and reproducible structure. The surface of the wild-type eye invariably forms a smooth, curved edge. Many *four-jointed* animals have eyes which resemble wild-type. Some animals with *four-jointed* mutations have disruptions in the structure of this tissue. Selected examples of animals that demonstrate the range of defects we have observed are shown (B–D). For all panels, anterior is left and dorsal is up.

developmental events that give rise to this phenotype difficult to perform.

Sequence Analysis of fj

The sequence of the *fj* transcript suggests that it encodes a novel cell surface or secreted protein. *fj* cDNAs contain a single large open reading frame encoding a predicted protein product of 583 amino acids. Codon usage within this open reading frame is consistent with it being a translated sequence in *Drosophila*. The nucleotide sequence preceding the putative initiator methionine (C A A A ATG) matches the *Drosophila* consensus sequence for translation initiation sites (Cavener, 1987). Comparison of this sequence with database entries did not identify any previously described sequences with a high degree of similarity. However, hydropathy analysis (Kyte and Doolittle, 1982) of the open reading frame revealed a potential transmembrane domain (underlined in Fig. 10). The absence of an N-terminal region that resembles known signal sequences suggests that this hydrophobic domain might act as both a transmembrane domain and an internal signal sequence, as found in type II transmembrane proteins (Singer, 1990). These proteins have a small, N-terminal intracellular domain and a large, C-terminal extracellular domain. In some proteins, such as tumor necrosis factor and the protein product of the *Drosophila hedgehog* gene, the C-terminal extracellular domain is cleaved, resulting in a secreted protein (Pennica *et al.*, 1984; Kriegler *et al.*, 1988; Lee *et al.*, 1994). Two potential sites for signal peptidase cleavage (von Heijne, 1986) are located within the transmembrane domain. In addition, the C-terminal region of *fj* contains several dibasic sites (Barr, 1991) that could be used as cleavage sites to produce a secreted protein.

As discussed below, the observation that *fj* is required for the development of the first three tarsal segments, but that the transcript is only detectable in the first tarsal segment, suggests that *fj* is required for the production of a signal from the first to the second and third tarsal segments. Although the sequence does not place *fj* in a previously characterized protein family, the presence of a predicted internal signal sequence indicates that *fj* could act to directly mediate cell–cell signaling in imaginal discs.

DISCUSSION

Enhancer Trap Screening in the F1 Generation

In many tissues, the localized activity of developmentally important genes is transcriptionally controlled. Enhancer trap screens provide an important tool for identifying and studying such genes (O'Kane and Gehring, 1987). This approach can complement genetic screens by identifying genes whose absence causes lethality prior to the stage of interest or whose function is obscured by the partially redundant action of other genes. In addition, specific reporter gene expression patterns can reveal how patterns of transcription are organized in groups of cells which do not exhibit obvious differences in morphology. Once identified, these lines provide a means to assay position-specific cell identities during development or following various environmental or genetic manipulations.

In this study, we have used the mini-*white* and *lacZ* genes to carry out a systematic screen for differences in gene regulation in the *Drosophila* eye disc. In a large-scale enhancer trap screen, two time-consuming steps are the establishment of *Drosophila* stocks from the transposant individuals and the isolation and staining of imaginal discs from those lines. The mini-*white* reporter allowed us to prescreen many adult transposants and limit further analysis to less than 1% of the total. The *lacZ* reporter allowed a more detailed analysis of enhancer activity during eye develop-

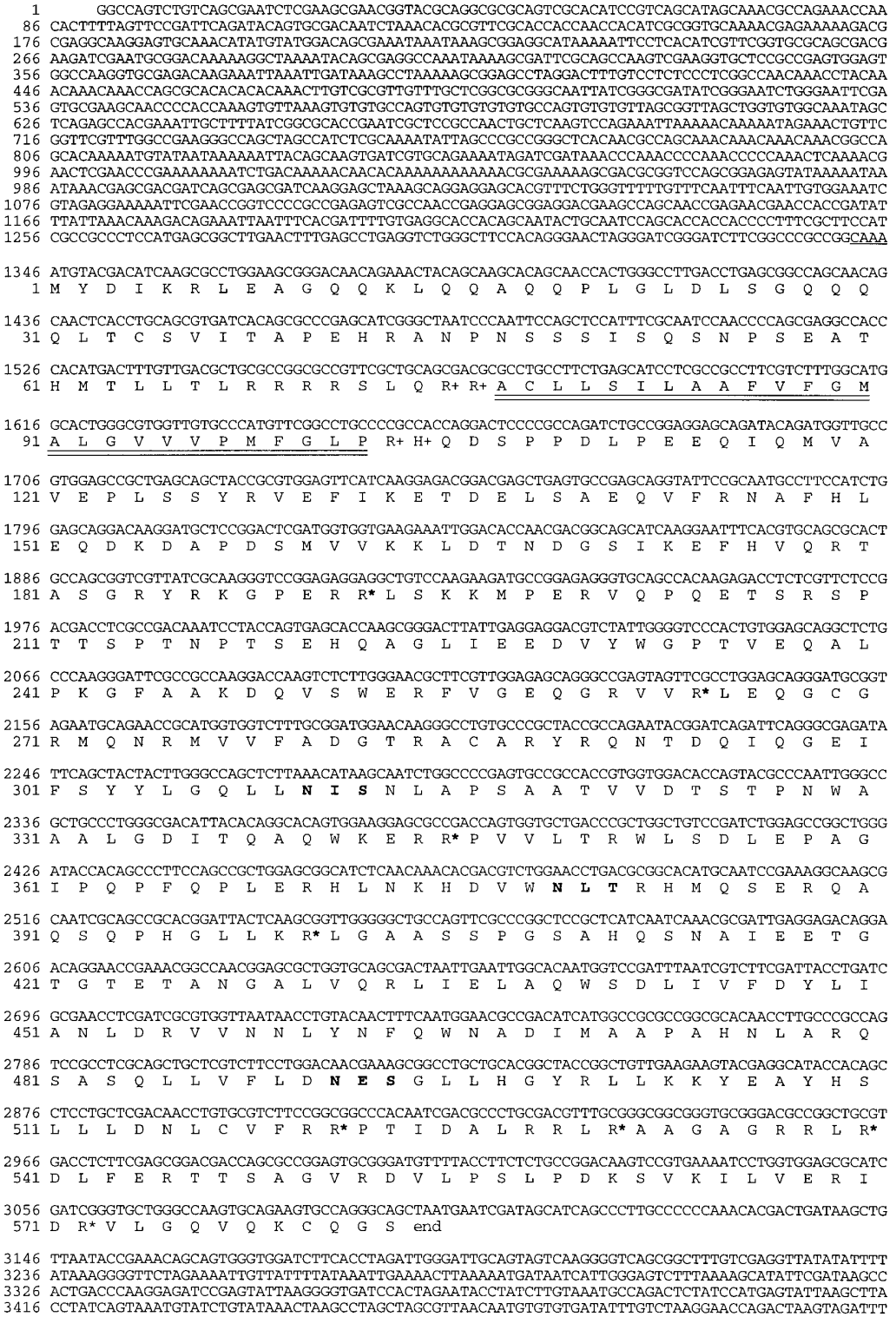

FIG. 10. *four-jointed* cDNA sequence. The amino acid sequence of the single long open reading frame is shown below the *four-jointed* cDNA nucleotide sequence. A perfect match to the *Drosophila* translation initiation consensus sequence is underlined next to the predicted start codon (Cavener, 1987). A potential polyadenylation signal (Proudfoot ,1991) near the end of the cDNA sequence is underlined. A hydrophobic region of the predicted peptide sequence extending from position 77 to position 102 is double underlined. The presence of two basic residues immediately before and after the hydrophobic region is indicated by a plus next to the amino acid symbols. The location of this hydrophobic region combined with the absence of an N-terminal signal sequence suggests that it acts as an internal signal sequence. This sequence is predicted to result in a large extracellular domain C-terminal to the hydrophobic region. Three potential N-linked glycosylation sites within this region are in bold type. There are several potential dibasic sites (Barr, 1991) which could act as cleavage sites to release part of the C-terminal region from the cell surface. These sites are indicated by asterisks.

ment. Almost half of these lines demonstrated a corresponding pattern of *lacZ* expression, confirming the usefulness of using two reporters.

Two factors may explain why some transposants with differences in adult eye pigmentation along the d-v axis did not show *lacZ* expression in the eye disc. First, we expect that some enhancers only activate reporter gene expression after third instar when *lacZ* expression was examined. Second, the *lacZ* promoter is presumed to possess an extremely low basal activity (Bier *et al.,* 1989) while the mini-*white* promoter has some, but not all, of the *cis*-acting sequences required for wild-type expression of the *white* gene (Pirrotta *et al.,* 1985; Pirrotta and Rastelli, 1994). The difference in promoters may make the mini-*white* reporter more sensitive to enhancer activity in the eye. In addition, the mini-*white*, but not *lacZ*, promoter should also be sensitive to negative enhancer elements or silencers.

Organization of Positional Information in the Eye Disc

Based on a previous analysis of axon guidance in the *Drosophila* visual system, we believed that photoreceptor cells would have distinct positional identities along the d-v axis of the developing eye disc. In this study, we have described differential reporter gene expression along the d-v axis of the developing *Drosophila* eye. In general, enhancer trap lines often reflect the expression pattern of endogenous genes. We have identified one gene, *fj*, which shows graded expression across the d-v axis of the developing eye, directly demonstrating transcriptional differences in this tissue. In addition, transcripts associated with two other loci described here have also been identified (M.H.B. and H.S., unpublished results; H. McNeill and M. Simon, personal communication). Thus, analysis of reporter expression patterns can reveal how patterns of transcriptional activation are organized in the developing eye.

The expression patterns we have described suggest that there are many transcriptionally distinct positions along the d-v axis of the eye disc. We find that expression of reporter genes at cytological positions 69D or 24D is restricted to dorsal or ventral sectors of the eye disc. In between these regions, there is small group of cells that do not express either reporter. We have also described graded expression of reporter genes inserted at 53C and 55C, with the highest expression levels near the equator (i.e., the d-v midline) and lower levels near the dorsal or ventral poles. Thus, the d-v position of a developing ommatidium can be approximately defined by its location in the dorsal or ventral region of the disc and by its distance from the d-v midline.

These lines allow us to ask if position-specific identities arise early during disc growth or if they are only specified after the disc has approached its full size at the end of the third instar. The results of two recent studies (Zheng *et al.,* 1995; Chanut and Heberlein, 1995) suggest that signals required for the dorsal or ventral specific chirality and rotation of developing ommatidia might arise concurrently with ommatidial differentiation in the late third instar eye disc. In addition, one study (Chanut and Heberlein, 1995) found that induction of an ectopic morphogenetic furrow could alter the expression pattern of two d-v-specific lines described in this study. We have examined reporter gene expression patterns in less mature, smaller eye discs. In these discs, the pattern of reporter expression (dorsal, ventral, or equatorial) is essentially the same as observed in discs that are much larger, demonstrating that distinct transcriptional patterns are present in the eye disc well before ommatidial differentiation begins.

The expression patterns we report are reminiscent of patterns of gene activity described in models for the development of other discs (Meinhardt, 1982; Gelbart, 1989). In the developing leg and wing, the disc is subdivided into lineage compartments which show differential patterns of gene expression early in disc development. Recent studies have demonstrated that signals at the boundaries of these regions act to organize positional information across the disc (reviewed in Blair, 1995; Campbell and Tomlinson, 1995). The division of the eye disc into dorsal and ventral compartment-like regions was previously suggested by the analysis of cell clones in the eye (Baker, 1978; Waitz and Campos-Ortega, 1978). However, the intermingling of cells at the boundary between these regions (Ready *et al.,* 1976; Waitz and Campos-Ortega, 1978) does not conform to descriptions of compartment boundaries in other discs (Garcia *et al.,* 1973). Our data are consistent with an early division of the disc into dorsal and ventral regions of gene expression. By analogy to models for the development of other discs, it is possible that the boundaries of these regions (either the d-v midline or the periphery of the disc) provide signals that create gradients of gene expression during eye development. The position-specific markers described in this study provide an important tool for future experiments to evaluate such models.

Graded Expression of the fj Gene in the Developing Eye

Because of the central role of gradients in models for the development of positional information and topographic maps, we chose to further analyze P-element insertions at cytological position 55C which show an equatorial-to-polar gradient of *lacZ* expression. We have identified a transcribed region adjacent to the P-element insertions with an expression pattern similar to that seen with the *lacZ* reporter. The identification of this transcript clearly demonstrates that the *Drosophila* eye, like its vertebrate counterpart, has graded gene expression among cells at the same stage of development.

Several results indicate that this transcript is required for the function of the *fj* gene. In a separate study, deletions that affect this transcript were associated with *fj* mutations (Villano and Katz, 1995). We show that P-element insertions at this locus cause a decrease in *fj* gene activity. Several insertions associated with mild *fj* phenotypes are found at the 5′ end of the transcript and the insertion with the

strongest phenotype is located within the 5′ untranslated region. For two examples tested, removal of the P-element can lead to reversion of the associated *fj* phenotype. Deletion mutations that no longer contain any P-element sequences and remove part of the transcribed region are associated with strong *fj* mutations. Finally, the restricted expression of this transcript along the proximal–distal axis of the developing leg is consistent with the segment-specific defects in longitudinal growth of the adult leg seen in *fj* mutants.

Although our initial interest in *fj* arose from its expression pattern in the eye, our analysis of *fj* mutants has not revealed a highly penetrant eye phenotype. The low penetrance and variability of the deformed eye phenotype that we have described currently makes analysis of *fj* in this tissue difficult. However, the expression and phenotype of *fj* in the leg does provide useful information about how this gene acts during development.

fj Is Required for Cell–Cell Interactions in the Developing Leg

The phenotype of *fj* mutants indicates that this gene is required for the development of the proximal–distal (p-d) axis in the leg. Fate mapping of the leg disc shows that the future distal tip of the leg is in the center of the disc and that more proximal segments occupy a series of concentric rings within the disc (Cohen, 1993). During pupation, the leg disc telescopes outward to form the p-d axis of the adult leg. The original fj^1 mutation was described as causing a decrease in longitudinal growth (i.e., along the p-d axis) of some leg segments (Waddington, 1943; Tokunaga and Gerhart, 1976). We find that weak alleles affect development of the second and third tarsal segments and that strong alleles also affect development of the femur, the tibia, and the first tarsal segment. No *fj* allele has been described that affects the fourth and fifth tarsal segments. There does not appear to be a significant change in growth or patterning around the circumference of the leg in *fj* mutant animals. Among the strong alleles we have characterized is one deletion that includes the beginning of the predicted *fj* protein coding region, suggesting that the strong alleles reveal a null phenotype. Thus, *fj* is required for longitudinal growth of specific segments in the leg.

Several other genes required for the development of the p-d axis have been shown to have localized expression along the p-d axis (Campbell *et al.*, 1993; Cohen, 1993; Godt *et al.*, 1993; Mardon *et al.*, 1994) The segment-specific effects of weak and strong alleles of *fj* indicates that it may have nonuniform action along the p-d axis. Ideally, mosaic analysis would provide an indication of which parts of the developing leg require *fj* function. The results of a previous mosaic analysis of *fj* indicate that *fj* mutations have a cell nonautonomous effect over a short distance around the circumference of the leg (Tokunaga and Gerhart, 1976). However, this work did not distinguish in which segments *fj* acts during development of the tarsal region of the leg because large leg clones included cells from multiple tarsal segments. We have examined the expression of *fj* during leg development and find that the *fj* transcript is found in two concentric rings, consistent with a role in development of the p-d axis. Within the tarsal region of the leg, *fj* is required for the normal development of the first three tarsal segments, but the *fj* transcript is only observed in the first tarsal segment. We have also examined *lacZ* expression in several enhancer trap lines at the *fj* locus that gave rise to strong *lacZ* expression (data not shown). In the tarsal region, *lacZ* expression is restricted to the first tarsal segment in the third instar disc through 6 hr of pupal life, at which point the fusion of tarsal segments two and three can be clearly seen in *fj* mutant animals. Although we cannot rule out the possibility of extremely low levels of expression in tarsal segments two and three, our observations strongly suggest that the *fj* gene has a cell nonautonomous effect on the development of these segments. This effect is not simply a secondary consequence of a decrease in the size of tarsal segment one since some alleles of *fj* affect growth of tarsal segments two and three, but have no obvious effect on tarsal segment one. Thus, *fj* appears to be required to send a developmental signal from tarsal segment one to tarsal segments two and three.

In principle, the *fj* gene could encode a protein expressed in the first tarsal segment which provides a signal to the second and third segments or it might act to regulate the production of such a signal in the first tarsal segment. Sequence analysis of *fj* cDNAs indicates that it encodes a novel protein with a potential internal signal sequence. Villano and Katz have shown that a *fj* cDNA can direct synthesis of both secreted and transmembrane proteins in a mammalian *in vitro* translation system (Villano and Katz, 1995). During *Drosophila* leg development, the *fj* gene product could act as a transmembrane protein or it could be cleaved to generate a secreted protein. These results are consistent with *fj* encoding a protein that directly mediates cell–cell signaling. Understanding how a *fj*-dependent signal acts to influence leg growth will require a more detailed analysis of the cellular responses to this signal.

Role of fj during Eye Development

In contrast to the analysis of *fj* function in the leg, the relationship between the graded expression of *fj* in the eye disc and its phenotype in the adult eye is unclear. Examination of adult eyes from *fj* animals reveals irregularities in the curvature of the eye surface which occur with low penetrance. One possible explanation for the lack of a more severe eye phenotype is that a second system exists which can partially compensate for the absence of *fj* function during eye development. A number of genes identified on the basis of their *in vitro* activities or expression patterns do not show striking phenotypes when removed genetically. Genetic screens for ''synthetic lethals'' has identified pairs of genes with partially redundant functions in yeast (Guarente, 1993). In mice and flies, several genes whose absence results in apparently subtle developmental defects have been shown to have more fundamental roles by making

double mutants with genes having overlapping expression. In the case of *fj* mutants, it is possible that other molecules can either directly substitute for the absence of *fj* function in the eye or might act in parallel pathways which can compensate for removal of *fj*. It was previously reported (Waddington, 1943) that animals with mutations in both *fj* and another ''leg gene'' called *dachous* had a dramatic reduction of eye tissue, but we have not been able to confirm this result (M.H.B. and H.S., unpublished results). Ectopic expression of *fj* or combinations of *fj* mutations with other mutations affecting eye or leg development may provide a better understanding of how *fj* acts during the construction of the visual system.

In the developing *Drosophila* embryo, genetic screens have been extremely successful in identifying genes whose patterned expression is required for proper development (Nüsslein-Volhard, 1991). However, genetic approaches may have some limitations when single genes have multiple functions or when multiple genes have overlapping functions. Identification of such genes may require other techniques. In this study, an enhancer trap screen allowed the identification of a gene whose eye phenotype alone may not have led to the description of its gradient of expression. The characterization of *fj* described here provides a step toward understanding how patterned gene expression is generated and utilized during the development of the *Drosophila* leg and visual system.

ACKNOWLEDGMENTS

We thank E. Gateff for communicating her observation of P-*lacW* lines with nonuniform pigmentation; Sarah Wiesbrock for the initial identification of an insertion at 53C; K. Mejia for help isolating cDNA clones; D. Smith for help with the confocal microscope; E. Selig for help with the scanning election microscope; G. Rubin, F. Kafatos, and R. Davis for providing libraries; the Indiana stock center for providing *Drosophila* stocks; and J. Agapite and J. Klemm for comments on the manuscript. M.H.B was partially supported by an N.S.F. predoctoral fellowship. H.S. is an Associate Investigator of the Howard Hughes Medical Institute.

REFERENCES

Baier, H., and Bonhoeffer, F. (1992). Axon guidance by gradients of a target-derived component. *Science* 255, 472–475.

Baker, W. K. (1978). A clonal analysis reveals early developmental restrictions in the *Drosophila* head. *Dev. Biol.* 62, 447–463.

Barr, P. J. (1991). Mammalian subtilisins: the long-sought dibasic processing endoproteases. *Cell* 66, 1–3.

Bellen, H. J., O'Kane, C., Wilson, C., Grossniklaus, U., Pearson, R. K., and Gehring, W. J. (1989). P-element-mediated enhancer detection: A versatile method to study development in *Drosophila. Genes Dev.* 3, 1288–1300.

Bier, E., H., Vaessin, Shepherd, S., Lee, K., McCall, K., Barbel, S., Ackerman, L., Carretto, R., Uemura, T., Grell, E., Jan, L. Y., and Jan, Y. N. (1989). Searching for pattern and mutation in the *Drosophila* genome with a P-*lacZ* vector. *Genes Dev.* 3, 1273–1287.

Blair, S. S. (1995). Compartments and appendage development in *Drosophila. BioEssays* 17, 299–309.

Bonhoeffer, F., and Gierer, A. (1984). How do retinal axons find their targets on the tectum? *Trends Neurosci.* 7, 378–381.

Bryant, P. J. (1978). Pattern formation in imaginal discs. *In* ''The Genetics and Biology of *Drosophila*'' (M. Ashburner, and T. R. F. Wright, Eds.), pp. 229–335. Academic Press, London.

Campbell, G., and Tomlinson, A. (1995). Initiation of the proximodistal axis in insect legs. *Development* 121, 619–628.

Campbell, G., Weaver, T., and Tomlinson A. (1993). Axis specification in the developing *Drosophila* appendage: The role of *wingless*, *decapentaplegic*, and the homeobox gene *aristaless*. *Cell* 74, 1113–1123.

Cavener, D. R. (1987). Comparison of the consensus sequence flanking translational start sites in *Drosophila* and vertebrates. *Nucleic Acids Res.* 15, 1353–1361.

Chanut, F., and Heberlein, U. (1995). Role of the morphogenetic furrow in establishing polarity in the *Drosophila* eye. *Development*, in press.

Cheng, H.-J., Nakamoto, M., Bergemann, A. D., and Flanagan, J. G. (1995). Complementary gradients in expression and binding of ELF-1 and Mek4 in development of the topographic retinotectal projection map. *Cell* 82, 371–381.

Cohen, S. M. (1993). Imaginal disc development. *In* ''The Development of *Drosophila melanogaster*'' (M. Bate and A. Martinez-Arias, Eds.), pp. 474–517. Cold Spring Harbor Laboratory Press, Cold Spring Harbor, New York.

Crick, F. H., and Lawrence, P. A. (1975). Compartments and polyclones in insect development. *Science* 189, 340–347.

Deitcher, D. L., Fekete, D. M., and Cepko, C. L. (1994). Asymmetric expression of a novel homeobox gene in vertebrate sensory organs. *J. Neurosci.* 14, 486–498.

Drescher, U., Kremoser, C., Handwerker, C., Loschinger, J., Noda, M., and Bonhoeffer, F. (1995). In vitro guidance of retinal ganglion cell axons by RAGS, a 25 kDa tectal protein related to ligands for Eph receptor tyrosine kinases. *Cell* 82, 359–370.

Engels, W. R. (1989). P Elements in *Drosophila melanogaster*. *In* ''Mobile DNA''(D. E., Berg and H. M. Howe, Eds.), pp. 437–484. Am. Soc. Microbiol., Washington DC.

Fischbach, K.-F., and Dittrich, A. P. M. (1989). The optic lobe of *Drosophila melanogaster*. I. A Golgi analysis of wild-type structure. *Cell Tissue Res.* 258, 441–475.

Fraser, S. E. (1992). Patterning of retinotectal connections in the vertebrate visual system. *Curr. Opin. Neurobiol.* 2, 83–87.

Garcia, B. A., Ripoll, P., and Morata, G. (1973). Developmental compartmentalisation of the wing disk of *Drosophila. Nature New Biol.* 245, 251–253.

Gelbart, W. M. (1989). The *decapentaplegic* gene: a TGF-beta homologue controlling pattern formation in *Drosophila*. *Development* (Suppl.) 65–74.

Gierer, A. (1987). Direction cues for growing axons forming the retinotectal projection. *Development* 101, 479–489.

Godt, D., Couderc, J. L., Cramton, S. E., and Laski, F. A. (1993). Pattern formation in the limbs of *Drosophila: bric a brac* is expressed in both a gradient and a wave-like pattern and is required for specification and proper segmentation of the tarsus. *Development* 119, 799–812.

Guarente, L. (1993). Synthetic enhancement in gene interaction: A genetic tool come of age. *Trends Genet.* 9, 362–366.

Hazelrigg, T., and Petersen, S. (1992). An unusual genomic position effect on *Drosophila white* gene expression: Pairing dependence, interactions with *zeste*, and molecular analysis of revertants. *Genetics* 130, 125–138.

Holt, C. E., and Harris, W. A. (1993). Position, guidance, and mapping in the developing visual system. *J. Neurobiol.* 24, 1400–1422.

Jan, L. Y., and Jan, Y. N. (1982). Antibodies to horseradish peroxidase as specific neuronal markers in *Drosophila* and in grasshopper embryos. *Proc. Natl. Acad. Sci. USA* 79, 2700–2704.

Kaprielian, Z., and Patterson, P. H. (1994). The molecular basis of retinotectal topography. *BioEssays* 16, 1–11.

Kriegler, M., Perez, C., DeFay, K., Albert, I., and Lu, S. D. (1988). A novel form of TNF/cachectin is a cell surface cytotoxic transmembrane protein: ramifications for the complex physiology of TNF. *Cell* 53, 45–53.

Kunes, S., and Steller, H. (1993). Topography in the *Drosophila* visual system. *Curr. Opin. Neurobiol.* 3, 53–59.

Kunes, S., Wilson, C., and Steller, H. (1993). Independent guidance of retinal axons in the developing visual system of *Drosophila*. *J. Neurosci.* 13, 752–767.

Kyte, J., and Doolittle, R. F. (1982). A simple method for displaying the hydropathic character of a protein. *J. Mol. Biol.* 157, 105–132.

Lee, J. J., Ekker, S. C., Kessler, D. P. von, Porter, J. A., Sun, B. I., and Beachy, P. A. (1994). Autoproteolysis in *hedgehog* protein biogenesis. *Science* 266, 1528–1537.

Levis, R., Hazelrigg, T., and Rubin, G. M. (1985). Effects of genomic position on the expression of transduced copies of the *white* gene of *Drosophila*. *Science* 229, 558–561.

Lindsley, D. L., and Zimm,G. G. (1992). ''The Genome of *Drosophila melanogaster*.'' Academic Press, San Diego.

Mardon, G., Solomon, N. M., and Rubin, G. M. (1994). *dachshund* encodes a nuclear protein required for normal eye and leg development in *Drosophila*. *Development* 120, 3473–3486.

Masucci, J. D., Miltenberger, R. J., and Hoffmann, F. M. (1990). Pattern-specific expression of the *Drosophila decapentaplegic* gene in imaginal disks is regulated by 3′ cis-regulatory elements. *Genes Dev.* 4, 2011–2023.

McCaffrery, P., Posch, K. C., Napoli, J. L., Gudas, L., and Drager, U. C. (1993). Changing patterns of the retinoic acid system in the developing retina. *Dev. Biol.* 158, 390–399.

Meinertzhagen, I. A. (1973). Development of the compound eye and optic lobe of insects. *In* ''Developmental Neurobiology of Arthropods'' (D. Young, Ed.), pp. 51–104. Cambridge Univ. Press, Cambridge.

Meinhardt, H. (1982). ''Models of Biological Pattern Formation.'' Academic Press, London.

Morata, G., and Lawrence, P. A. (1977). The development of *wingless*, a homeotic mutation of *Drosophila*. *Dev. Biol.* 56, 227–240.

Moses, K., Ellis, M. C., and Rubin, G. M. (1989). The *glass* gene encodes a zinc-finger protein required by *Drosophila* photoreceptor cells. *Nature* 340, 531–536.

Moses, K., and Rubin, G. M. (1991). *glass* encodes a site-specific DNA-binding protein that is regulated in response to positional signals in the developing *Drosophila* eye. *Genes Dev.* 5, 583–593.

Nornes, H. O., Dressler, G. R., Knapik, E. W., Deutsch, U., and Gruss, P. (1990). Spatially and temporally restricted expression of Pax2 during murine neurogenesis. *Development* 109, 797–809.

Nüsslein-Volhard, C. (1991). Determination of the embryonic axes of *Drosophila*. (Suppl.) 1–10.

O'Kane, C. J., and Gehring,W. J. (1987). Detection *in situ* of genomic regulatory elements in *Drosophila*. *Proc. Natl. Acad. Sci. USA* 84, 9123–9127.

Pennica, D., Nedwin, G. E., Hayflick, J. S., Seeburg, P. H., Derynck, R., Palladino, M. A., Kohr, W. J., Aggarwal, B. B., and Goeddel, D. V. (1984). Human tumour necrosis factor: precursor structure, expression and homology to lymphotoxin. *Nature* 312, 724–729.

Pirrotta, V., and Rastelli, L. (1994). *White* gene expression, repressive chromatin domains and homeotic gene regulation in *Drosophila*. *BioEssays* 16, 549–556.

Pirrotta, V., Steller, H., and Bozzetti, M. P. (1985). Multiple upstream regulatory elements control the expression of the *Drosophila white* gene. *EMBO J.* 4, 3501–3508.

Proudfoot, N. (1991). Poly(A) signals. *Cell* 64, 671–674.

Ready, D. F., Hanson, T. E., and Benzer, S. (1976). Development of the *Drosophila* retina, a neurocrystalline lattice. *Dev. Biol.* 53, 217–240.

Rissi, M., Wittbrodt, J., Delot, E., Naegeli, M., and Rosa, F. M. (1995). Zebrafish Radar: A new member of the TGF-beta superfamily defines dorsal regions of the neural plate and the embryonic retina. *Mech. Dev.* 49, 223–234.

Robertson, H. M., Preston, C. R., Phillis, R. W., Johnson-Schlitz, D. M., Denz, W. K., and Engels, W. R. (1988). A stable genomic source of P-element transposase in *Drosophila melanogaster*. *Genetics* 118, 461–470.

Sanes, J. R. (1993). Topographic maps and molecular gradients. *Curr. Opin. Neurobiol.* 3, 67–74.

Savitt, J. M., Trisler, D., and Hilt, D. C. (1995). Molecular cloning of TOPAP: A topographically graded protein in the developing chick visual system. *Neuron* 14, 253–261.

Selleck, S. B., and Steller, H. (1991). The influence of retinal innervation on neurogenesis in the first optic ganglion of *Drosophila*. *Neuron* 6, 83–99.

Singer, S. J. (1990). The structure and insertion of integral proteins in membranes. *Annu. Rev. Cell. Biol.* 6, 247–296.

Spencer, F. A., Hoffmann, F. M., and Gelbart, W. M. (1982). *Decapentaplegic*: A gene complex affecting morphogenesis in *Drosophila melanogaster*. *Cell* 28, 451–461.

Sperry, R. W. (1963). Chemoaffinity in the orderly growth of nerve fiber patterns and connections. *Proc. Natl. Acad. Sci. USA* 50, 703–710.

Steller, H., and Pirrotta, V. (1986). P transposons controlled by the heat shock promoter. *Mol. Cell. Biol.* 6, 1640–1649.

Tautz, D., and Pfeifle, C. (1989). A nonradioactive *in situ* hybridization method for the localization of specific RNAs in *Drosophila* embryos reveals a translational control of segmentation gene *hunchback*. *Chromosoma* 98, 81–85.

Tokunaga, C., and Gerhart, J. C. (1976). The effect of growth and joint formation on bristle pattern in *D. melanogaster*. *J. Exp. Zool.* 198, 79–95.

Tomlinson, A. (1988). Cellular interactions in the developing *Drosophila* eye. *Development* 104, 183–193.

Trujillo, C. O., and Melamed, J. (1973). The development of the retina–lamina complex in muscoid flies. *J. Ultrastruct. Res.* 42, 554–581.

Udin, S. B., and Fawcett, J. W. (1988). Formation of topographic maps. *Annu. Rev. Neurosci.* 11, 289–327.

Villano, J. L., and Katz, F. N. (1995). *four-jointed* is required for intermediate growth in the proximal-distal axis in *Drosophila*. *Development* 121, 2767–2777.

von Heijne, G. (1986). A new method for predicting signal sequence cleavage sites. *Nucleic Acids Res.* 14, 4683–4690.

Waddington, C. H. (1943). The development of some ''leg genes'' in *Drosophila*. *J. Genet.* 45, 29–43.

Waitz, M., and Campos-Ortega, J. A. (1978). Cell clones and pattern formation: Developmental restrictions in the compound eye of *Drosophila*. *Wilhelm Roux's Arch. Dev. Biol.* 184, 155–170.

Wilson, C., Pearson, R. K., Bellen, H. J., O'Kane, C. J., Grossniklaus,

U., and Gehring, W. J. (1989). P-element-mediated enhancer detection: An efficient method for isolating and characterizing developmentally regulated genes in *Drosophila*. *Genes Dev*. 3, 1301–1313.

Winberg, M. L., Perez, S. E., and Steller, H. (1992). Generation and early differentiation of glial cells in the first optic ganglion of *Drosophila melanogaster*. *Development* 115, 903–911.

Wolpert, L. (1969). Positional information and the spatial pattern of cellular differentiation. *J. Theor. Biol.* 25, 1–47.

Zheng, L., Zhang, J., and Carthew, R. W. (1995). *frizzled* regulates mirror-symmetric pattern formation in the *Drosophila* eye. *Development* 121, 3045–3055.

Received for publication September 18, 1995
Accepted November 2, 1995